Science Advances
AAAS

advances.sciencemag.org/cgi/content/full/7/4/eabd8637/DC1

Supplementary Materials for

Axodendritic versus axosomatic cochlear efferent termination is determined by afferent type in a hierarchical logic of circuit formation

Jemma L. Webber, John C. Clancy, Yingjie Zhou, Natalia Yraola, Kazuaki Homma, Jaime García-Añoveros*

*Corresponding author. Email: anoveros@northwestern.edu

Published 20 January 2021, *Sci. Adv.* **7**, eabd8637 (2021)
DOI: 10.1126/sciadv.abd8637

This PDF file includes:

Supplementary Materials

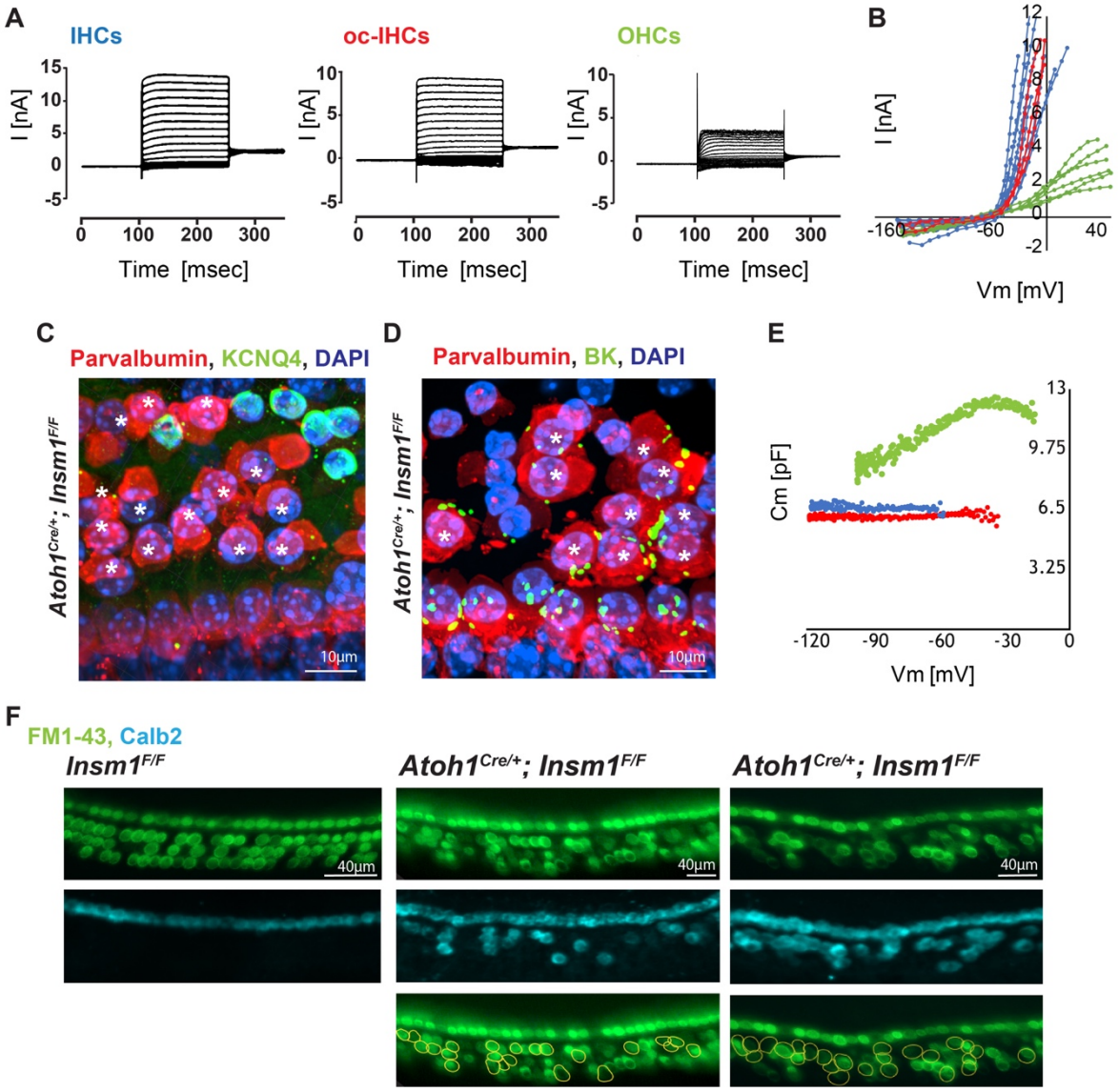

Figure S1. oc-IHCs display the same physiological properties as IHCs.
A,B) Whole cell recordings reveal that oc-IHCs lack small Ik,n (KCNQ4-mediated) characteristic of OHCs and instead display the IHC-characteristic Ik,f (BK-mediated). Examples of voltage-dependent whole-cell currents recorded in IHCs (blue), oc-IHCs (red) and OHCs (green) are shown in (A) and current-voltage (I-V) relationships summarized in B.
C,D) Immunohistochemistry confirms that oc-IHCs do not express KCNQ4 potassium channels as control OHCs do (C), but instead express BK potassium channels like IHCs (D).
E) Representative recordings of cell membrane electric capacitance (Cm). The capacitance changes characteristic of electromotile OHCs (green) are not detected in oc-IHCs (red) or IHCs (blue). Visual observation confirmed that while all (n=17) recorded OHCs were electromotile, none of the oc-IHCs (n=6) or of the IHCs (n=10) were electromotile.
F) FM1-43 uptake reveals that oc-IHCs mechanotransduce. FM1-43 enters hair cells through their mechanotransduction channel (69). Cochlear explants were incubated with FM1-43 for 20sec before washout and imaging. IHCs, OHCs and oc-IHCs were labelled, but other cells in the cochlea were not. Transformed cells (oc-IHCs) were revealed by a post-fix and immunostaining for Calb2, which differentially labels IHCs and oc-IHCs vs. OHCs in the *Insm1* cKOs (middle right panels), and are indicated by a yellow outline in the bottom panels.

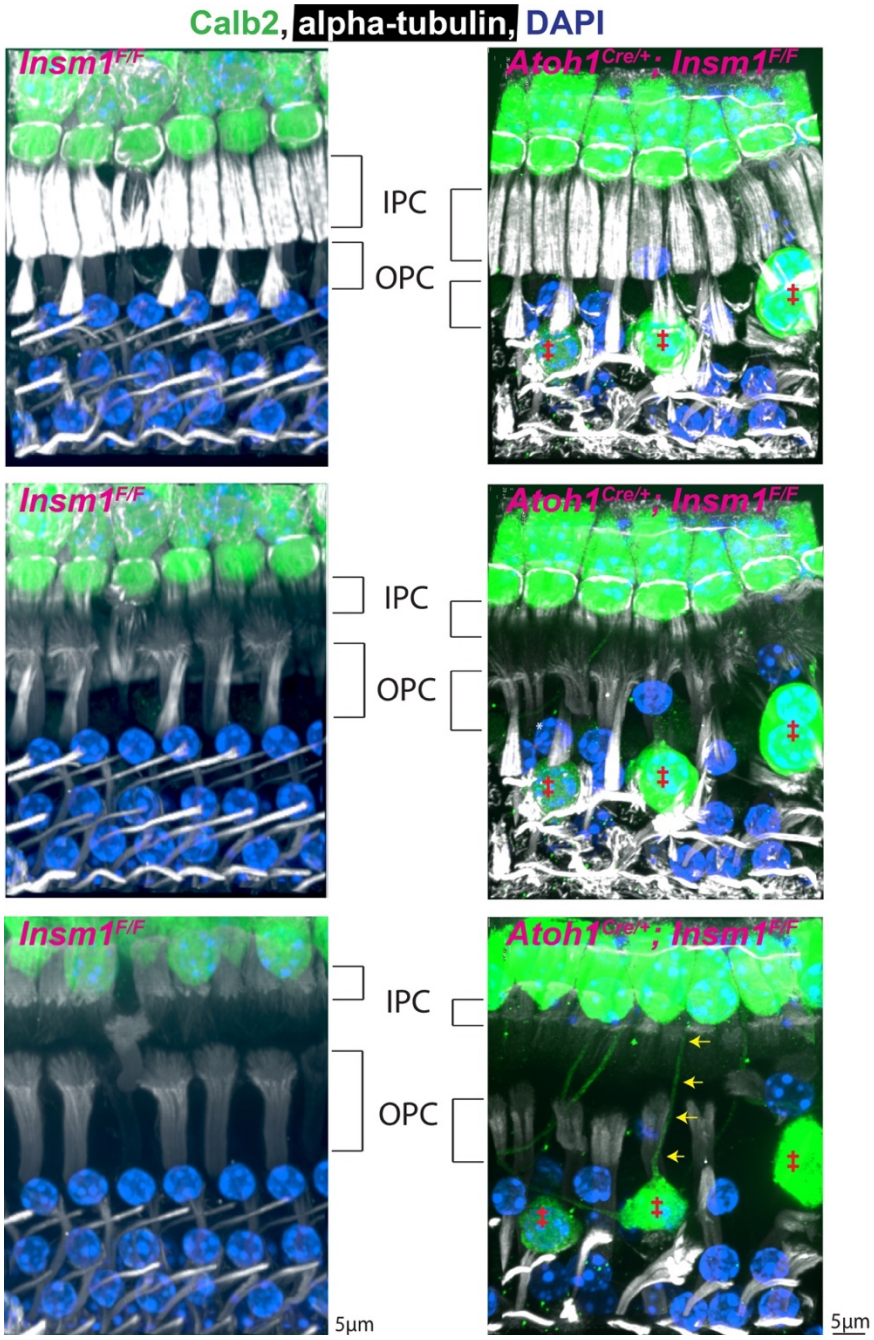

Figure S2. oc-IHCs are separated from the tunnel of Corti and inner compartment.
A top view of whole mount control and *Insm1* cKO cochlea (middle turn) with alpha-tubulin labelling IPCs, OPCs and DCs. The lower panels have the top (more apical) sections removed to better visualize the IPC and OPC columnar processes (middle panels) and Calb2 labelled type I afferent fibers crossing into the outer compartment (lower panel, red arrows).

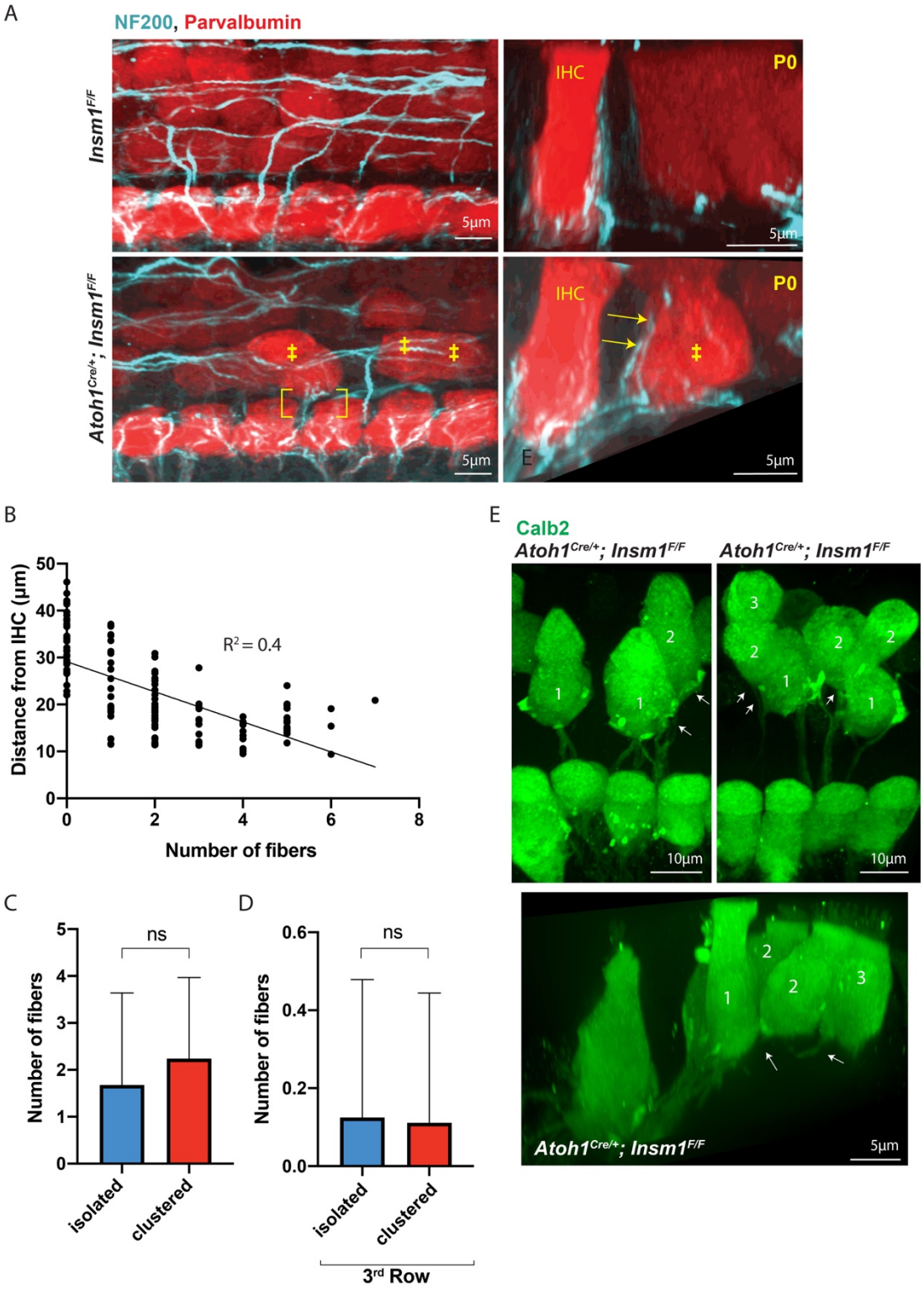

Figure S3. Innervation of oc-IHCs is already apparent by birth, and is independent of clustering and only weakly correlated with distance from the IHCs.

A) Whole mount views of P0 control and mutant cochlea (middle turns) immunostained for parvalbumin to label hair cells (with higher intensity staining in the IHCs and oc-IHCs relative to OHCs), and neurofilament 200 (NF200) to label all fibers. In control animals all fibers that cross into the outer compartment are determined to be type II afferents as they turn towards the base. In contrast, fibers are observed to cross into the outer compartment (brackets in top view and arrows in side view) when oc-IHCs are present (denoted by a ‡).

B) The number of type I afferent fibers that innervate an oc-IHC is weakly correlated with the relative distance from the row of IHCs to the oc-IHC ($R^2 = 0.4$, n=123).
C,D) The average number of type I afferent fibers that reach an oc-IHC is not significantly different for oc-IHCs that are in isolation i.e. surrounded by wildtype OHCs (isolated, blue bar) vs. oc-IHCs surrounded by neighboring oc-IHCs (clustered, red bar). The graph in C) shows data for all oc-IHCs (n=147, p=0.3, students unpaired t-test), while D) is plotted using data only from third row oc-IHCs (n=17, p=0.9, students unpaired t-test). Error bars represent standard deviation. E) Whole mount top and side views of *Insm1* cKO cochleae (from middle turns) provide additional examples of second and third row oc-IHCs that receive at least one Calb2 positive type I afferent fiber. The row number is given for each individual oc-IHC.

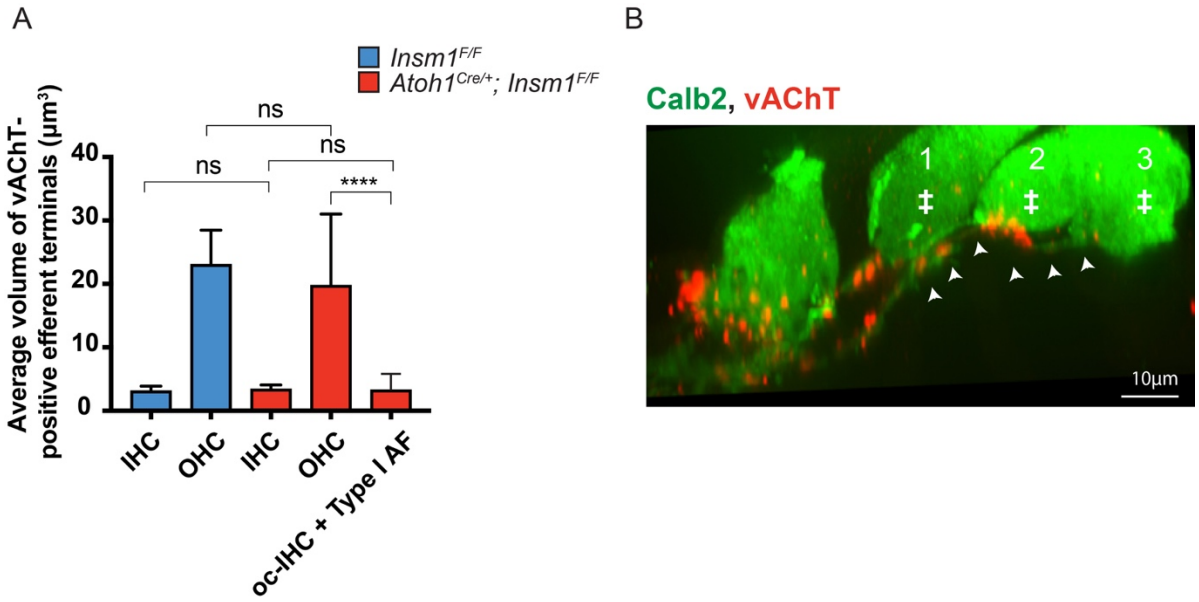

Figure S4. Efferent boutons (vAChT+) terminating near oc-IHCs have the small volume characteristic of those terminating near IHCs.

A) Quantification of the volumes of individual vAChT-positive efferent terminals associated with IHCs, OHCs and oc-IHCs. The average volumes of terminals associated with mutant IHCs and OHCs were indistinguishable from those observed in control animals (N≥23, One-way ANOVA, followed by Tukey's multiple comparisons test; IHCs control vs. mutant, $p>0.999$; OHCs control vs. mutant, $p=0.5256$). vAChT-positive efferent terminals observed close to oc-IHCs that were innervated by a type I afferent fiber were small in size, and indistinguishable from those observed in IHCs (Innervated oc-IHCs vs. IHCs, $p>0.999$) and significantly different from OHCs (innervated oc-IHCs vs. OHCs, <0.0001). Error bars represent standard deviation.

B) An additional example of a second and third row oc-IHC that each receive a type I afferent fiber with associated axodendritic efferent termination. Side view of an *Insm1* cKO cochlea (middle turn) immunolabeled for Calb2 (green) and vAChT (red) to distinguish type I afferent fibers and efferent terminals, respectively. ‡ denotes oc-IHCs with the corresponding row number labelled above.

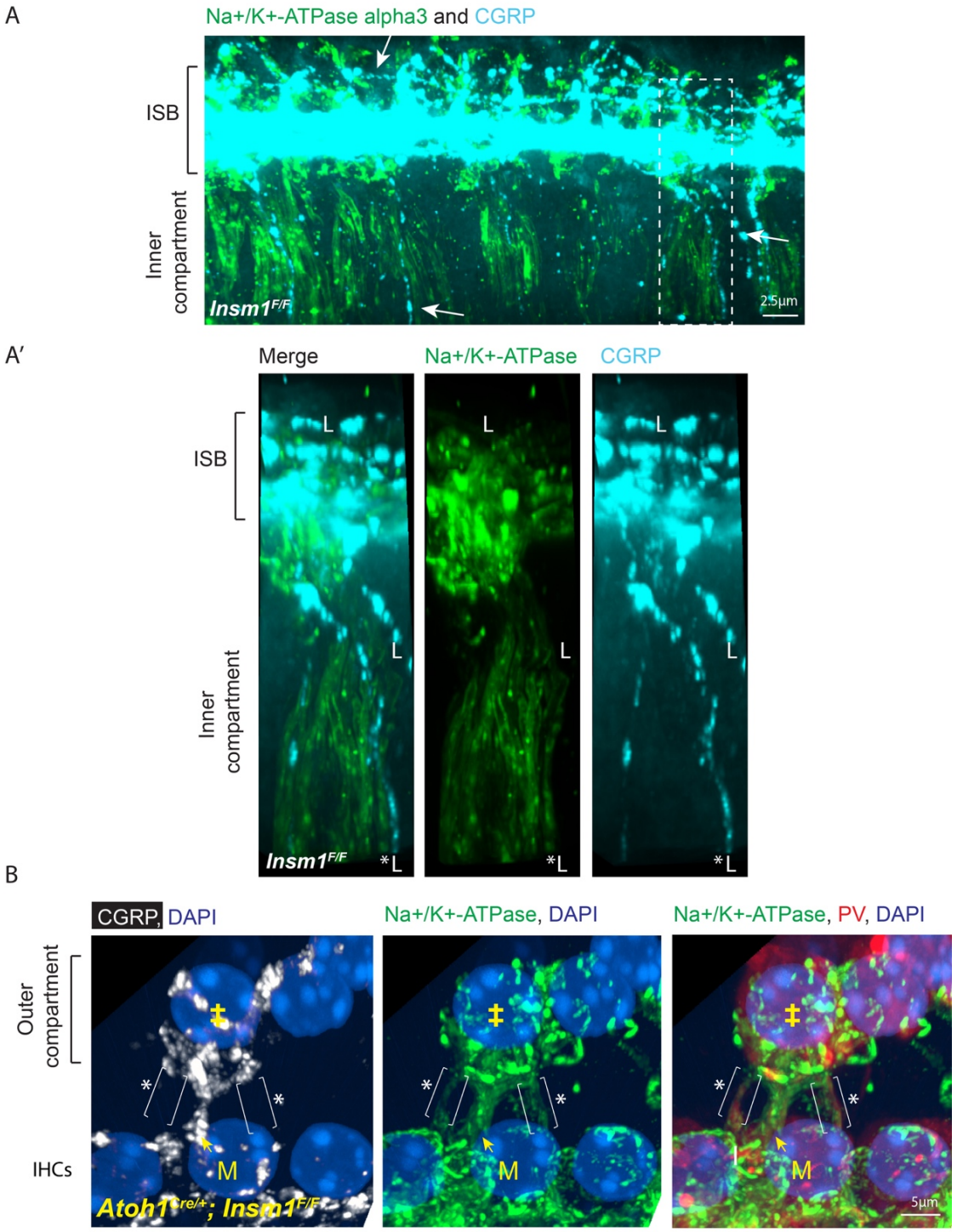

Figure S5. Immunohistochemistry for CGRP and Na^+/K^+-ATPase alpha 3 distinguish LOC efferent from type I afferent fibers.

A, A') Whole mount view of radial fibers projecting towards and spiraling in the ISB, under the IHCs, of a middle turn from a control adult (*Insm1*$^{F/F}$) cochlea. Fibers were immunostained with antibodies against Na^+/K^+-ATPase alpha 3 (labelling MOCs and type I afferents in green) and CGRP (labelling all efferent fibers in cyan). The dashed line indicates the region magnified in A' (top-view). In A, arrows point to radial and ISB CGRP-labeled fibers that are not co-labeled with Na^+/K^+-ATPase alpha 3, and are thus LOC fibers (CGRP+/ATPase-). In A', the CGRP+/ATPase- LOCs are indicated with an (L), while the asterisk (*) indicates one of the many type I afferents that are CGRP-/ATPase+.

B) Top view of an adult *Insm1* cKO cochlea with Na^+/K^+-ATPase alpha 3 labelling MOCs and type I afferents (green) and CGRP labelling all efferent fibers (white). Parvalbumin labels IHCs and oc-IHCs with greater intensity than OHCs. Type I fibers (*), outlined with brackets projecting to the oc-IHC (‡), are labelled by Na^+/K^+-ATPase alpha 3, and not CGRP, while a MOC fiber reaching the oc-IHC is labelled by both (yellow arrow, M).

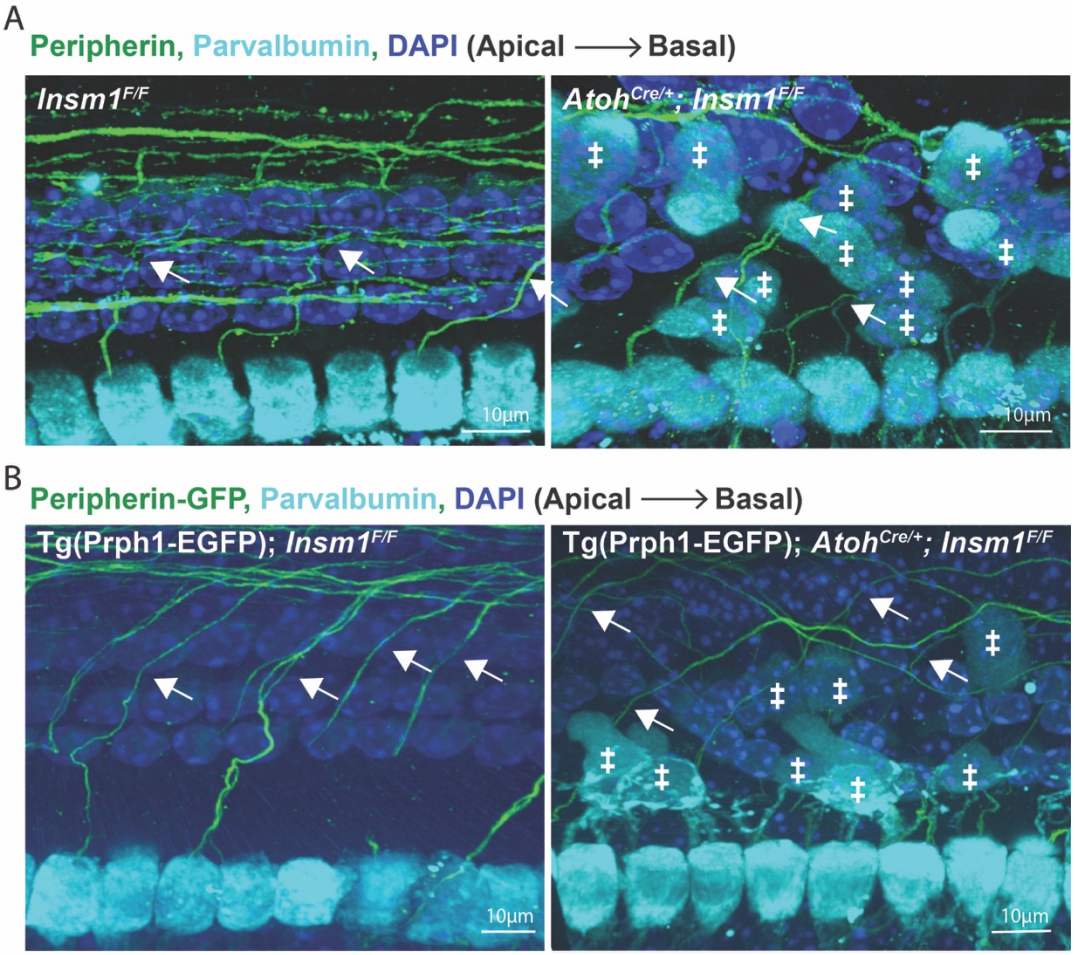

Figure S6. Peripherin labelled type II fibers cross into the outer compartment and turn towards the base.

Whole mount view of cochlea from A) P7 *Insm1*$^{F/F}$ and *Atoh1*$^{Cre/+}$*; Insm1*$^{F/F}$ or B) P10 Tg(Prph1-EGFP); *Insm1*$^{F/F}$ and Tg(Prph1-EGFP); *Atoh1*$^{Cre/+}$*; Insm1*$^{F/F}$ animals. Arrows depict peripherin (A) or peripherin-GFP (B) labelled type II fibers that cross into the outer compartment and turn correctly towards the base in both control and mutant cochlea, despite the presence of oc-IHCs (denoted by ‡) in the mutant.

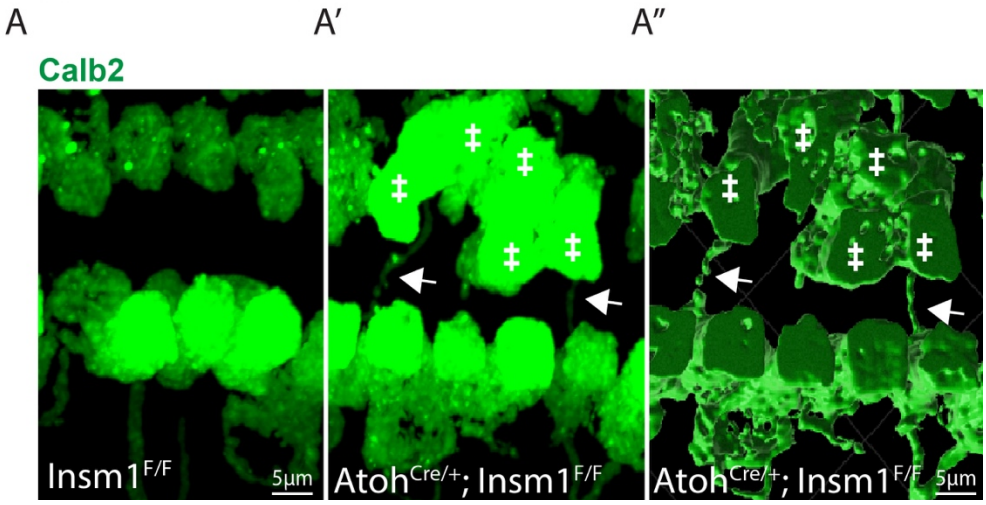

Figure S7. Afferent fibers innervate oc-IHCs in the absence of efferent fibers.
Whole mount view of cochlear explants cultured at P2, prior to the arrival of efferent fibers in the outer compartment. Explants were fixed and stained for Calb2 after 6DIV. In explants from control mice, Calb2 positive fibers do not cross into the outer compartment, as expected (A). In explants from *Insm1* cKOs, Calb2 positive fibers cross into the outer compartment to innervate oc-IHCs (A' and 3D construction in A''), as they do in intact mutant animals.

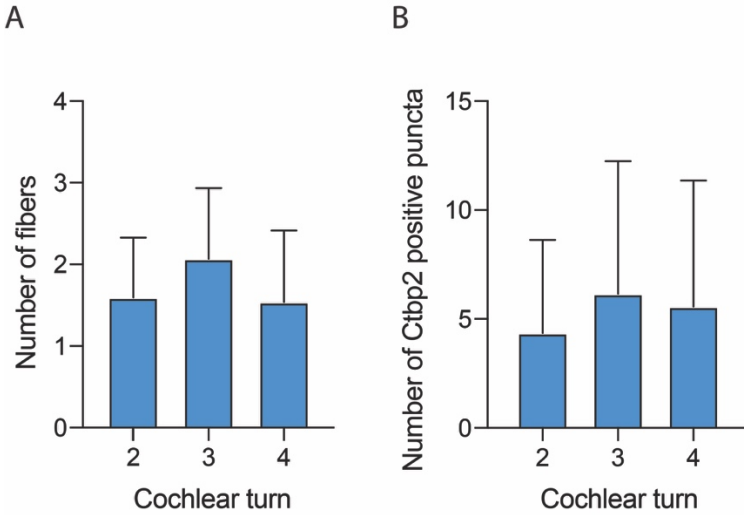

Figure S8. Type I afferents contact oc-IHCs in a manner that is primarily independent of tonotopic location. The number of A) Calb2-positive type I afferent fibers contacting oc-IHCs or B) CtBP2 positive puncta were counted per cochlear turn (where 1 is the most apical, and 4 is the most basal). A Kruskal-Wallis test followed by Dunn's multiple comparisons revealed no significant differences ($p>0.4$). N= at least 4 independent cochleae counted.

Feature	IHCs	OHCs	oc-IHCs	Reference
Fgf8 mRNA	Present	Absent	Present	Wiwatpanit et al. (40)
Bcl11b	Absent	Present	Absent	Wiwatpanit et al. (40)
Rprm mRNA	High	Low	High	Wiwatpanit et al. (40)
Tbx2 mRNA	Present	Absent	Present	Wiwatpanit et al. (40)
Id4 mRNA	High	Low	High	Wiwatpanit et al. (40)
Brip1 mRNA	Present	Absent	Present	Wiwatpanit et al. (40)
Car13 mRNA	Present	Absent	Present	Wiwatpanit et al. (40)
Pink1 mRNA	Present	Absent	Present	Wiwatpanit et al. (40)
Lrrn1 mRNA	Present	Absent	Present	Wiwatpanit et al. (40)
Neuroplastin at stereocilia	Low	High	Low	Wiwatpanit et al. (40)
VGlut3	Present	Absent	Present	Wiwatpanit et al. (40)
Calmodulin	High	Low	High	Wiwatpanit et al. (40)
Oncomodulin	Undetected	Present	Undetected	Wiwatpanit et al. (40)
Prestin	Absent	Present	Absent	Wiwatpanit et al. (40)
Calb2	High	Low	High	Fig. 2, this study
Parvalbumin >P7	High	Low	High	Fig. 6, this study
Ribeye (CtBP2) puncta	Multiple puncta (more than 1-2)	1-2 puncta, absent from nucleus	Multiple puncta (more than 1-2)*	Wiwatpanit et al. (40); Fig. 3, this study
CtBP2 in nucleus	Present	Undetected	Present	Wiwatpanit et al. (40); Fig. 3, this study
GluR2/3 puncta	Apposed to CtBP2	Mainly absent	Apposed to CtBP2*	Fig. 3, this study

Stereocilia	Straight and long	V-shaped and short	Straight and long	Wiwatpanit et al. (40)
Cell shape	Flask shape	Cylindrical	Flask shape	Wiwatpanit et al. (40)
Nuclear size	Large	Small	Large	Wiwatpanit et al. (40)
BK expression	Present	Undetected	Present	Fig. S1, this study
KCNQ4 expression	Undetected	Present	Undetected	Fig. S1, this study
Potassium currents	Ik,f-mediated	Ik,n-mediated	Ik,f-mediated	Fig. S1, this study
Electromotility	No	Yes	No	Fig. S1, this study

Table S1. Transformed cells display all known features tested of IHCs and lack all known features tested of OHCs.

REFERENCES AND NOTES

1. H. Spoendlin, Anatomy of cochlear innervation. *Am. J. Otolaryngol.* **6**, 453–67 (1985).

2. P. Dallos, Neurobiology of cochlear hair cells, in *Auditory Physiology and Perception*, Y. Cazals, K. Horner, L. Demany, Eds. (Elsevier, 1992), pp. 3–17.

3. J. Zheng, W. Shen, D. Z. He, K. B. Long, L. D. Madison, P. Dallos, Prestin is the motor protein of cochlear outer hair cells. *Nature* **405**, 149–155 (2000).

4. M. C. Liberman, J. Gao, D. Z. Z. He, X. Wu, S. Jia, J. Zuo, Prestin is required for electromotility of the outer hair cell and for the cochlear amplifier. *Nature* **419**, 300–304 (2002).

5. H. Liu, J. L. Pecka, Q. Zhang, G. A. Soukup, K. W. Beisel, D. Z. Z. He, Characterization of transcriptomes of cochlear inner and outer hair cells. *J. Neurosci.* **34**, 11085–11095 (2014).

6. J. Waldhaus, R. Durruthy-Durruthy, S. Heller, Quantitative high-resolution cellular map of the organ of Corti. *Cell Rep.* **11**, 1385–1399 (2015).

7. J. C. Burns, M. C. Kelly, M. Hoa, R. J. Morell, M. W. Kelley, Single-cell RNA-seq resolves cellular complexity in sensory organs from the neonatal inner ear. *Nat. Commun.* **6**, 8557 (2015).

8. M. W. Kelley, E. C. Driver, C. Puligilla, Regulation of cell fate and patterning in the developing mammalian cochlea. *Curr. Opin. Otolaryngol. Head Neck Surg.* **17**, 381–387 (2009).

9. A. C. Meyer, T. Frank, D. Khimich, G. Hoch, D. Riedel, N. M. Chapochnikov, Y. M. Yarin, B. Harke, S. W. Hell, A. Egner, T. Moser, Tuning of synapse number, structure and function in the cochlea. *Nat. Neurosci.* **12**, 444–453 (2009).

10. A. V. Bulankina, T. Moser, Neural circuit development in the mammalian cochlea. *Physiology (Bethesda)* **27**, 100–112 (2012).

11. A. M. Berglund, D. K. Ryugo, Hair cell innervation by spiral ganglion neurons in the mouse. *J. Comp. Neurol.* **255**, 560–570 (1987).

12. W. B. Warr, Organization of olivocochlear efferent systems in mammals, in *The Mammalian Auditory Pathway: Neuroanatomy*, D. B. Webster, A. N. Popper, R. R. Fay, Eds. (Springer New York, 1992), pp. 410–448.

13. D. D. Simmons, Development of the inner ear efferent system across vertebrate species. *J. Neurobiol.* **53**, 228–250 (2002).

14. A. B. Elgoyhen, E. Katz, The efferent medial olivocochlear-hair cell synapse. *J. Physiol. Paris* **106**, 47–56 (2012).

15. M. M. Frank, L. V. Goodrich, Talking back: Development of the olivocochlear efferent system. *Wiley Interdiscip. Rev. Dev. Biol.* **7**, e324 (2018).

16. B. R. Shrestha, L. V. Goodrich, Wiring the cochlea for sound perception, in *The Oxford Handbook of the Auditory Brainstem*, K. Kandler, Ed. (Oxford Univ. Press, 2019), Chapter 1, pp. 1–40.

17. H. Yang, X. Xie, M. Deng, X. Chen, L. Gan, Generation and characterization of Atoh1-Cre knock-in mouse line. *Genesis* **48**, 407–413 (2010).

18. Y.-S. Lee, F. Liu, N. Segil, A morphogenetic wave of p27Kip1 transcription directs cell cycle exit during organ of Corti development. *Development* **133**, 2817–2826 (2006).

19. P. Chen, J. E. Johnson, H. Y. Zoghbi, N. Segil, The role of Math1 in inner ear development: Uncoupling the establishment of the sensory primordium from hair cell fate determination. *Development* **129**, 2495–2505 (2002).

20. E. J. Koundakjian, J. L. Appler, Goodrich LV. Auditory neurons make stereotyped wiring decisions before maturation of their targets. *J. Neurosci.* **27**, 14078–14088 (2007).

21. W. Y. Kim, B. Fritzsch, A. Serls, L. A. Bakel, E. J. Huang, L. F. Reichardt, D. S. Barth, J. E. Lee, NeuroD-null mice are deaf due to a severe loss of the inner ear sensory neurons during development. *Development* **128**, 417–426 (2001).

22. T. M. Coate, S. Raft, X. Zhao, A. K. Ryan, E. B. Crenshaw, M. W. Kelley, Otic mesenchyme cells regulate spiral ganglion axon fasciculation through a Pou3f4/EphA4 signaling pathway. *Neuron* **73**, 49–63 (2012).

23. T. M. Coate, N. A. Spita, K. D. Zhang, K. T. Isgrig, M. W. Kelley, Neuropilin-2/Semaphorin-3F-mediated repulsion promotes inner hair cell innervation by spiral ganglion neurons. *eLife* **4**, (2015).

24. L.-C. Huang, P. R. Thorne, G. D. Housley, J. M. Montgomery, Spatiotemporal definition of neurite outgrowth, refinement and retraction in the developing mouse cochlea. *Development* 2007 **134**, 2925–2933.

25. N. R. Druckenbrod, L. V. Goodrich, Sequential retraction segregates SGN processes during target selection in the cochlea. *J. Neurosci.* **35**, 16221–16235 (2015).

26. P. Vyas, J. S. Wu, A. Zimmerman, P. Fuchs, E. Glowatzki, Tyrosine hydroxylase expression in type II cochlear afferents in mice. *J. Assoc. Res. Otolaryngol.* **18**, 139–151 (2017).

27. P. Vyas, J. S. Wu, A. Jimenez, E. Glowatzki, P. A. Fuchs, Characterization of transgenic mouse lines for labeling type I and type II afferent neurons in the cochlea. *Sci. Rep.* **9**, 5549 (2019).

28. S. Maison, L. D. Liberman, M. C. Liberman, Type II cochlear ganglion neurons do not drive the olivocochlear reflex: Re-examination of the cochlear phenotype in peripherin knock-out mice. *Eneuro* **3**, ENEURO.0207–ENEU16.2016 (2016).

29. J. Defourny, A.-L. Poirrier, F. Lallemend, S. Mateo Sánchez, J. Neef, P. Vanderhaeghen, E. Soriano, C. Peuckert, K. Kullander, B. Fritzsch, L. Nguyen, G. Moonen, T. Moser, B. Malgrange, Ephrin-A5/EphA4 signalling controls specific afferent targeting to cochlear hair cells. *Nat. Commun.* **4**, 1438 (2013).

30. A. I. Lyuksyutova, C.-C. Lu, N. Milanesio, L. A. King, N. Guo, Y. Wang, J.Nathans, M. Tessier-Lavigne, Y. Zou, Anterior-posterior guidance of commissural axons by Wnt-frizzled signaling. *Science* **302**, 1984–1988 (2003).

31. K. Onishi, B. Shafer, C. Lo, F. Tissir, A. M. Goffinet, Y. Zou. Antagonistic functions of Dishevelleds regulate Frizzled3 endocytosis via filopodia tips in Wnt-mediated growth cone guidance. *J. Neurosci.* **33**, 19071–19085 (2013).

32. B. Shafer, K. Onishi, C. Lo, G. Colakoglu, Y. Zou, Vangl2 promotes Wnt/planar cell polarity-like signaling by antagonizing Dvl1-mediated feedback inhibition in growth cone guidance. *Dev. Cell* **20**, 177–191 (2011).

33. S. R. Ghimire, M. R. Deans, *Frizzled3* and *Frizzled6* cooperate with *Vangl2* to direct cochlear innervation by type II spiral ganglion neurons. *J. Neurosci.* **39**, 8013–8023 (2019).

34. S. M. Echteler, Developmental segregation in the afferent projections to mammalian auditory hair cells. *Proc. Natl. Acad. Sci. U.S.A.* **89**, 6324–6327 (1992).

35. A. L. Bergeron, A. Schrader, D. Yang, A. A. Osman, D. D. Simmons, The final stage of cholinergic differentiation occurs below inner hair cells during development of the rodent cochlea. *J. Assoc. Res. Otolaryngol.* **6**, 401–415 (2005).

36. A. Shnerson, C. Devigne, R. Pujol, Age-related changes in the C57BL/6J mouse cochlea. II. Ultrastructural findings. *Dev. Brain Res.* **2**, 77–88 (1981).

37. G. Kearney, J. Zorrilla de San Martín, L. G. Vattino, A. B. Elgoyhen, C. Wedemeyer, E. Katz, Developmental synaptic changes at the transient olivocochlear-inner hair cell synapse. *J. Neurosci.* **39**, 3360–3375 (2019).

38. R. Pujol, E. Carlier, C. Devigne, Different patterns of cochlear innervation during the development of the kitten. *J. Comp. Neurol.* **177**, 529–535 (1978).

39. Q. Ma, D. J. Anderson, B. Fritzsch, Neurogenin 1 null mutant ears develop fewer, morphologically normal hair cells in smaller sensory epithelia devoid of innervation. *J. Assoc. Res. Otolaryngol.* **1**, 129–143 (2000).

40. T. Wiwatpanit, S. M. Lorenzen, J. A. Cantú, C. Z. Foo, A. K. Hogan, F. Márquez, J. C. Clancy, M. J. Schipma, M. A. Cheatham, A. Duggan, J. García-Añoveros, Trans-differentiation of outer hair cells into inner hair cells in the absence of INSM1. *Nature* **563**, 691–695 (2018).

41. S. M. Lorenzen, A. Duggan, A. B. Osipovich, M. A. Magnuson, J. García-Añoveros, Insm1 promotes neurogenic proliferation in delaminated otic progenitors. *Mech. Dev.* **138**, 233–245 (2015).

42. B. R. Shrestha, C. Chia, L. Wu, S. G. Kujawa, M Charles Liberman, L. V. Goodrich, Sensory neuron diversity in the inner ear is shaped by activity. *Cell* **174**, 1229–1246.e17 (2018).

43. C. Petitpré, H. Wu, A. Sharma, A. Tokarska, P. Fontanet, Y. Wang, F. Helmbacher, K. Yackle, G. Silberberg, S. Hadjab, F. Lallemend, Neuronal heterogeneity and stereotyped connectivity in the auditory afferent system. *Nat. Commun.* **9**, 3691 (2018).

44. S. Sun, T. Babola, G. Pregernig, K. S. So, M. Nguyen, S.-S. M. Su, A. T. Palermo, D. E. Bergles, J. C. Burns, U. Müller, Hair cell mechanotransduction regulates spontaneous activity and spiral ganglion subtype specification in the auditory system. *Cell* **174**, 1247–1263.e15 (2018).

45. H. M. Sobkowicz, J. E. Rose, G. L. Scott, C. V. Levenick, Distribution of synaptic ribbons in the developing organ of Corti. *J. Neurocytol.* **15**, 693–714 (1986).

46. H. M. Sobkowicz, J. E. Rose, G. E. Scott, S. M. Slapnick, Ribbon synapses in the developing intact and cultured organ of Corti in the mouse. *J. Neurosci.* **2**, 942–957 (1982).

47. L. D. Liberman, M. C. Liberman, Postnatal maturation of auditory-nerve heterogeneity, as seen in spatial gradients of synapse morphology in the inner hair cell area. *Hear. Res.* **339**, 12–22 (2016).

48. F. A. Thiers, J. B. Nadol, M. C. Liberman, Reciprocal synapses between outer hair cells and their afferent terminals: Evidence for a local neural network in the mammalian cochlea. *J. Assoc. Res. Otolaryngol.* **9**, 477–489 (2008).

49. M. C. Liberman, L. W. Dodds, S. Pierce, Afferent and efferent innervation of the cat cochlea: Quantitative analysis with light and electron microscopy. *J. Comp. Neurol.* **301**, 443–460 (1990).

50. M. C. Liberman, Morphological differences among radial afferent fibers in the cat cochlea: An electron-microscopic study of serial sections. *Hear. Res.* **3**, 45–63 (1980).

51. N. Y. Kiang, J. M. Rho, C. C. Northrop, M. C. Liberman, D. K. Ryugo, Hair-cell innervation by spiral ganglion cells in adult cats. *Science* **217**, 175–177 (1982).

52. H. Yang, J. Gan, X. Xie, M. Deng, L. Feng, X. Chen, Z. Gao, L. Gan, Gfi1-Cre knock-in mouse line: A tool for inner ear hair cell-specific gene deletion. *Genesis* **48**, 400–406 (2010).

53. K. N. Darrow, E. J. Simons, L. Dodds, M. C. Liberman, Dopaminergic innervation of the mouse inner ear: Evidence for a separate cytochemical group of cochlear efferent fibers. *J. Comp. Neurol.* **498**, 403–414 (2006).

54. W. J. McLean, K. A. Smith, E. Glowatzki, S. J. Pyott, Distribution of the Na,K-ATPase α subunit in the rat spiral ganglion and organ of Corti. *J. Assoc. Res. Otolaryngol.* **10**, 37–49 (2009).

55. S. F. Maison, R. B. Emeson, J. C. Adams, A. E. Luebke, M. C. Liberman, Loss of alpha CGRP reduces sound-evoked activity in the cochlear nerve. *J. Neurophysiol.* **90**, 2941–2949 (2003).

56. R. E. Perkins, D. K. Morest, A study of cochlear innervation patterns in cats and rats with the Golgi method and Nomarkski Optics. *J. Comp. Neurol.* **163**, 129–158 (1975).

57. D. D. Simmons, A transient afferent innervation of outer hair cells in the postnatal cochlea. *Neuroreport* **5**, 1309–1312 (1994).

58. M. C. Liberman, D. F. O'Grady, L. W. Dodds, J. McGee, E. J. Walsh,. Afferent innervation of outer and inner hair cells is normal in neonatally de-efferented cats. *J. Comp. Neurol.* **423**, 132–139 (2000).

59. C. Puligilla, F. Feng, K. Ishikawa, S. Bertuzzi, A. Dabdoub, A. J. Griffith, B. Fritzsch, M. W. Kelley, Disruption of fibroblast growth factor receptor 3 signaling results in defects in cellular differentiation, neuronal patterning, and hearing impairment. *Dev. Dyn.* **236**, 1905–1917 (2007).

60. M. M. Mellado Lagarde, B. C. Cox, J. Fang, R. Taylor, A. Forge, J. Zuo, Selective ablation of pillar and Deiters' cells severely affects cochlear postnatal development and hearing in mice. *J. Neurosci.* **33**, 1564–1576 (2013).

61. K. D. Zhang, T. M. Coate, Recent advances in the development and function of type II spiral ganglion neurons in the mammalian inner ear. *Semin. Cell Dev. Biol.* **65**, 80–87 (2017).

62. S. R. Ghimire, E. M. Ratzan, M. R. Deans, A non-autonomous function of the core PCP protein VANGL2 directs peripheral axon turning in the developing cochlea. *Development* **145**, dev159012 (2018).

63. R. M. Nemzou N, A V Bulankina, D. Khimich, A. Giese, T. Moser, Synaptic organization in cochlear inner hair cells deficient for the CaV1.3 (alpha1D) subunit of L-type Ca2+ channels. *Neuroscience* **141**, 1849–1860 (2006).

64. S. McLenachan, Y. Goldshmit, K. J. Fowler, L. Voullaire, T. P. Holloway, A. M. Turnley, P. A. Ioannou, J. P. Sarsero, Transgenic mice expressing the Peripherin-EGFP genomic reporter display intrinsic peripheral nervous system fluorescence. *Transgenic Res.* **17**, 1103–1116 (2008).

65. K.W. Beisel, S. M. Rocha-Sanchez, K. A. Morris, L. Nie, F. Feng, B. Kachar, E. N. Yamoah, B. Fritzsch Differential expression of KCNQ4 in inner hair cells and sensory neurons is the basis of progressive high-frequency hearing loss. *J. Neurosci.* 2005 **25**, 9285–93.

66. M. J. Fogarty, L. A. Hammond, R. Kanjhan, M. C. Bellingham, P. G. Noakes, A method for the three-dimensional reconstruction of Neurobiotin™-filled neurons and the location of their synaptic inputs. *Front. Neural Circuits* **7**, 153 (2013).

67. Santos-Sacchi J, Kakehata S, Takahashi S. Effects of membrane potential on the voltage dependence of motility-related charge in outer hair cells of the guinea-pig. *J. Physiol. Lond.* **510**, 225–235 (1998).

68. K. D. Haque, A. K. Pandey, M. W. Kelley, C. Puligilla, Culture of embryonic mouse cochlear explants and gene transfer by electroporation. *J. Vis. Exp.*, 52260 (2015).

69. J. R. Meyers, R. B. MacDonald, A. Duggan, D. Lenzi, D. G. Standaert, J. T. Corwin, D. P. Corey, Lighting up the senses: FM1-43 loading of sensory cells through nonselective ion channels. *J. Neurosci.* **23**, 4054–4065 (2003).